COMPACTION AND SWELLING OF Ca-SMECTITE IN WATER AND IN CaCl₂ SOLUTIONS: WATER ACTIVITY MEASUREMENTS AND MATRIX RESISTANCE TO COMPACTION

Jérôme H. Denis

Schlumberger Cambridge Research, PO Box 153
Cambridge CB3 OHG, United Kingdom

Abstract—Direct water-activity measurements were made for calcium-smectite-CaCl₂ mixtures. The samples used were prepared by high-pressure filtration and had water contents <0.60% by weight of clay. For deionized water, the water activity (aw) ranged between 1 and 0.4 and was independent of the pressure history of the clay cake. Good agreement was found with the results of an adsorption isotherm. Samples were also prepared in 1, 3, and 5 M CaCl₂ solutions. The final concentration of chloride present in the cakes was measured: substantial anion exclusion was observed. The water activity of the clay-salt mixtures depended on both the water content and the concentration of CaCl₂. The data can be well represented by the expression $aw = \min(aw_0, aw_c^* \times aw_s^*)$, where aw_0 is the water activity of the brine used to prepare the cake, and aw_c^* and aw_s^* are water activities calculated for clay (in absence of salt) and salt (in absence of clay), respectively. The compaction and swelling behavior of a core of the same Ca-smectite was also investigated for pressures (P) between 0.5 and 800 bar. In two compaction-swelling cycles total recovery of the void ratio (e) was observed with, however, large hysteresis in the relationship between e and P. The osmotic pressure developed in the core at equilibrium, evaluated using the water-activity data, was intermediate between the compaction and swelling pressures. Apparently, another force, P_m, linked to irreversible changes in the structure of the matrix was contributing to the resistance to compaction. P_m values agreed with literature results for Ca-smectite suspensions.

Key Words—Calcium chloride, Compaction, Matrix resistance, Rheology, Smectite, Swelling, Water activity.

INTRODUCTION

Smectite clays have been widely studied for their ability to disperse and form stable colloidal suspensions (see reviews by van Olphen, 1977; Hunter, 1987). Whereas this property can be advantageous in some industrial applications (e.g., drilling mud technology), the uptake of water by clay rocks and their subsequent swelling is a major problem in soil engineering, tunnelling operations, and oil well drilling. The long-range interactions between clay particles (typically for separations >50 Å) has been the subject of numerous studies. The DLVO theory gives a quantitative interpretation of the swelling of Na-smectite, but the hysteresis observed between the first compaction and the rebound indicates that other forces are involved in the behavior of clay gels (Warkentin *et al.*, 1957). For alkali ions, agreement between swelling results and theory decreases with the polarizability and the hydration energy of the counterion (Lubetkin *et al.*, 1984): this can be explained by a surface adsorption mechanism (Pashley, 1981); however, poor agreement has been found between experiment and theory for Ca-smectite (Warkentin *et al.*, 1957; Mesri and Olson, 1971), and modification of the DLVO to account for the experimental observations is an active research field (see, e.g. Kjellander and Marčelja, 1988; Kjellander *et al.*, 1988; Attard *et al.*, 1988). The short-range interaction between clay particles has also been widely studied. van

Olphen (1954) discussed interlayer forces in bentonite for small interlayer separations and showed that hydration effects become important, leading to deviation from the DLVO theory. X-ray powder diffraction measurements indicate that the interlayer separations of smectite change in a stepwise manner at low relative humidity (Glaeser and Méring, 1968), a phenomenon known as crystalline swelling. Direct forces measurements using the method developed by Israelachvili and Adams (1978) have also been used to investigate short range interactions between single sheets of mica. Comparison of experimental results for mica surfaces to the DLVO theory shows that the expected minimum in the interaction potential is not observed for electrolyte concentration higher than a threshold (Israelachvili and Adams, 1978; Pashley, 1981). In this regime, hydration and solvent ordering are predominant, and the force between two interacting mica sheets varies in an oscillatory manner with separation (Pashley and Israelachvili, 1984).

Thus, DLVO theory cannot describe crystalline swelling, and although significant progress has been made in understanding the phenomenon at a microscopic scale, the macroscopic properties of clay material have received less attention. Short-range interactions are of a paramont importance to the study of the properties of most shales and clay rocks, inasmuch as their water content is such that crystalline swelling is initially predominant. To give a better insight into
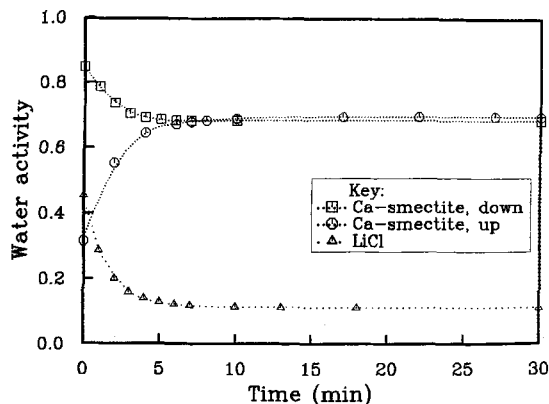
Figure 1. Time response of the humidity meter for a disc of compacted Ca-smectite and saturated LiCl. Note that starting the measurement from a sensor drier (up) or wetter (down) than the sample did not modify the equilibrium value.

the properties of concentrated clay materials, direct water activity measurements were made for the system Redhill smectite-$CaCl_2$. The compaction and swelling properties of an undisturbed core the same clay were also investigated. By relating composition, osmotic properties, and the compaction-swelling behavior, the part of the compaction stress directly supported by the matrix was estimated.

EXPERIMENTAL

Materials

The clay used in these experiments was the Redhill smectite, obtained from a Laporte Fuller's earth quarry in Redhill, Surrey, United Kingdom. The rock was micronized and the fraction passing a 100-μm sieve was used for the experiments. The smectite content was determined by XRD to be >95%. The nature of the exchangeable cations and the cation-exchange capacity (CEC) were determined by exchange with tetramethylammonium bromide. A CEC value of 84 meq/100 g and a counterion population containing a large predominance of Ca (>95%), with traces of Mg and K, were found. To measure the adsorption isotherms, a fraction of the material was washed in 0.3 M perchloric acid until a stable pH of 4 was obtained. The clay was then rinsed first in 0.5 M Ca-perchlorate and then in deionized water until salt free. The compaction and swelling behavior of the clay was investigated using a small, fully saturated core drilled perpendicularly to the bedding planes of the rock. The sample had a diameter of 24.04 mm and was 25.32 mm long; its initial water content was 20.3 wt. %. The calcium chloride used was Analar grade $CaCl_2 \cdot 6H_2O$ supplied by BDH. The water was deionized using a Milli-Q system until a resistivity of 18 MΩ cm^{-1} was obtained.

Methods

Water activity measurements. Compacted clay discs used in the water activity measurements were obtained by filtration in two hydraulic presses, the working ranges of which were 1–70 and 100–2000 bar. About 6 g of clay, suspended in 40 ml of the appropriate fluid, was used to prepare each disc. One end of the cell was closed with a porous disc covered with a filter paper of <5-μm pore diameter. The pressure was applied by a low-friction piston also fitted with a porous disc.

As the pressure was applied by mechanical means, the sample was drained by both ends. The compression of the samples was followed using a dial gauge. Once equilibrium was reached (generally after ~36 hr), the disc and the piston supporting the filters were extruded from the cell. The clay discs were then separated from the filters. To avoid spurious end effect, the surface of the sample was quickly scraped with a scalpel. These handling operations were performed with maximum speed, typically in less than 30 s, to minimize water-vapor exchanges with the atmosphere. The rate of water exchange, measured on a few samples, was <0.1 mg/s. As the sample weighed ~7 g, corrections for water uptake/loss were ignored. The sample was then divided in two subsamples, one of which was immediately weighed to determine the water content, taken as the weight loss after overnight drying at 200°C. This temperature was chosen because some of the materials prepared with concentrated brines retained significant amounts of water at lower temperatures. Weights were determined with an accuracy of 0.1 mg. The dried clay was kept for chloride determination.

The water activity was measured at 20 ± 0.1°C using a Humidat-TH2 humidity meter provided by Novasina. The instrument was calibrated using three saturated solutions of LiCl, $Mg(NO_3)_2$, and $BaCl_2$, the water activities of which were 0.113, 0.544, and 0.910, respectively. To limit water exchanges, the sample was enclosed in a small thermostated box. As the sensor measured vapor pressures, an equilibrium had to be reached between the air contained in the box and the porous clay disc. To verify this, measurements were made starting from low-humidity and high-humidity conditions by previously equilibrating the sensor with LiCl- and $BaCl_2$-saturated solutions, respectively. The results shown in Figure 1 clearly indicate that the same final equilibrium value was obtained. Furthermore, the equilibration time was comparable to that for a saturated salt solution. The influence of possible inhomogeneity of the discs was also tested by measuring the water activity of crushed samples. The value found using this method was slightly lower (0.02), but this difference may well have been due to partial drying during the grinding.

The $CaCl_2$ content of the cakes was obtained as follows: a known weight of clay, close to 1 g, was washed in 40 cm^3 of deionized water. After centrifugation for particle separation, the concentration of chloride was determined from the potential of a chloride specific electrode, using a Corning Ion Analyzer 250 and calomel reference electrode. The apparatus was previously calibrated using $CaCl_2$ standards in order to obtain the results directly in a concentration scale. The measurements were generally made in the concentration range 0.01–0.001 mole/liter, for which good Nernst response was observed, with slopes of about 44 mV per concentration decade. All measurements were duplicated, and the mean value was used. The overall precision, including the effect of the sample preparation, was about 6%.

From the weight loss, w_1, and the salt content, s, (both expressed as weight per weight of dry solid), the water content, w, (expressed as the weight per weight of dry clay) and the salt molality, m, of the pore fluid were calculated:

$$w = \frac{w_1}{1-s} \text{ and } m = \frac{s}{Mw_1}, \tag{1}$$

where M is the molal mass of $CaCl_2$. Assuming that the density of the pore fluid was unaffected by the clay, the porosity, ψ, and the void ratio, $e = \psi/(1-\psi)$, were calculated using a value of 2700 kg/m^3 for the clay density ρ_c, and the data compiled by Söhnel and Novotný (1985) for the brine density. The concentration of fixed charges in the compacted clay discs, A, was calculated as the ratio of the CEC, C, to the water content, w.
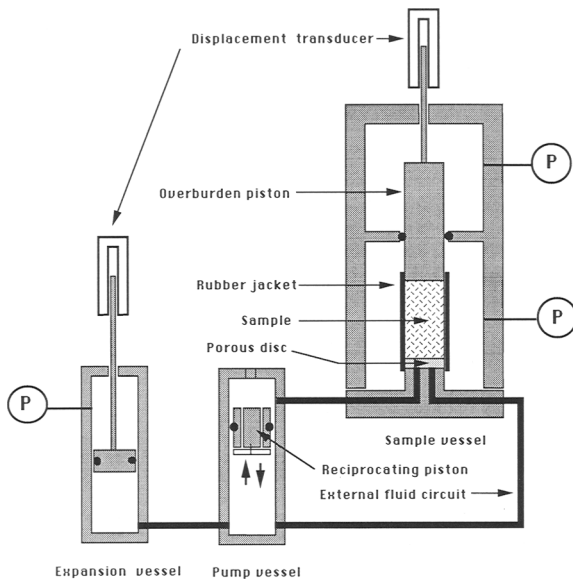
The water adsorption measurements were made at 20 ±

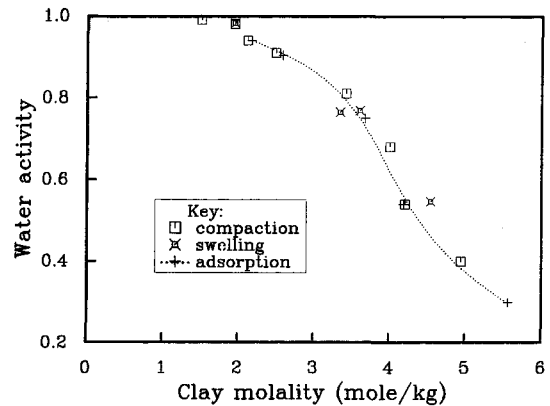Figure 2.   Schematic diagram of the compaction-swelling apparatus.

Figure 3.   Water activity vs. water content for Redhill smectite-water cakes, using the compaction and vapor-adsorption techniques. Swollen cakes were allowed to equilibrate at a pressure lower than the initial compaction pressure.

0.1°C by equilibrating in the chamber of the humidity meter ~80 mg of clay with saturated solutions of LiCl, $CaCl_2 \cdot 6H_2O$, $Mg(NO_3)_2$, NaCl, and a 1 M solution of $CaCl_2$, the water activities of which were 0.11, 0.30, 0.54, 0.75 and 0.94, respectively (Young, 1967; Robinson and Stokes, 1970). When the relative humidity measured by the meter had stabilized at the value of the solution, the sample was weighed with a precision of ±0.02 mg at several intervals of time to verify that equilibrium had been reached. The water content was obtained by subtracting the sample dry weight determined at the end of the test after overnight heating at 200°C.

Compaction and swelling test. The compaction and swelling measurements were made in the high-pressure rig shown schematically in Figure 2. The rig consisted of three vessels to hold the sample, circulate the external fluid, and permit the expansion of the external fluid volume. The sample sat on a porous stainless steel disc and was submitted to an axial stress via a piston. A confining pressure was also applied through a rubber jacket by the confining oil. The axial stress was supplied by a system of pneumatic pumps, whereas the con-

fining pressure was controlled with a pressure amplifier and a spindle press. The pressures were measured using two types of transducers working in the ranges 0–60 and 60–1400 bar. The positions of the pistons in the sample and separator vessels were monitored with linear voltage-displacement transducers, the detection limit and accuracy of which were 3 and 10 μm, respectively. The data were logged by the same computer system used to control the pressures. The accuracy of the control was ±0.5 bar at low pressures and ±0.5% at high pressures. During the test, the stress conditions were nearly isotropic, although the overburden had to be kept slightly higher than the confining stress to ensure good contact between the sample and the piston. The external fluid phase was deionized water, the pressure of which was kept constant at 1 bar above atmospheric pressure. The water was circulated to avoid effects due to changes in the ionic composition of the fluid. This circulation induced small pressure pulsations: these affected the measurement of the bulk volume variation made by monitoring the position of the piston in the separator vessel. To solve this problem, the pump was stopped at the end of each pressure step. The pressure was then adjusted exactly to 1 bar before recording the position of the piston.

At the end of each pressure step, the equilibrium void ratio e was calculated from the change in volume of the external fluid ΔV, and the characteristics of the sample. The axial deformation, Δl, was obtained from the displacement of the piston in the sample vessel and, combined with ΔV, gave the average change in radius:

$$\Delta R = \frac{\Delta V - \pi R^2 \Delta l}{2\pi l R}, \qquad (2)$$

where the radius R is calculated at the end of the preceding pressure step. At the end of the experiment, the water content and physical dimensions of the sample were measured. The values obtained agreed within ±1% with those derived from the volume and length variations. Two successive compaction and swelling cycles were made, their maximum pressures being 200 and 800 bar, respectively.

RESULTS AND DISCUSSION

Water activity measurements

Ca-smectite/water system. The water contents, void ratios, and water activities obtained for deionized water are listed in Table 1. The water activity, aw, is also plotted as a function of the clay molality, A, in Figure
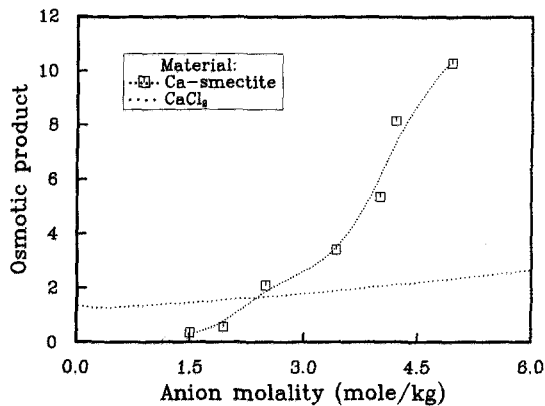
Table 1.   Void ratio, clay molality and water activity as functions of compaction pressure for the Ca smectite-water cakes.[1]

P_c (bar)	Void ratio	Clay molality (mole/kg)	Water activity
30	1.51	1.50	0.99
166	0.91	2.49	0.91
582	0.66	3.42	0.81
1040	0.56	4.00	0.68
1564	0.54	4.20	0.54
2084	0.46	4.94	0.40
'free'	1.17	1.94	0.98
832	0.68	3.34	0.77
1040	0.63	3.60	0.77
1560	0.50	4.54	0.55

[1] Data above the line are for normally consolidated cakes, data below the line are for swollen cakes (see text).

Figure 4. Osmotic product calculated for Redhill smectite and $CaCl_2$. Data for $CaCl_2$ are from Rard *et al.* (1977).

3. A sharp decrease of aw was observed for A > 2 mole/kg, reaching a value of 0.40 for A = 5 mole/kg.

Experimental work has shown that the first compaction-swelling cycle presents large hysteresis loops in the relationship between e and p (Warkentin *et al.*, 1957; Olson and Mesri, 1970). To check whether the water activity of water saturated clays depended on their void ratio only and not on their compression-swelling history, aw was also measured on samples swollen at equilibrium with a pressure less than the original compaction pressure. These results are also plotted in Figure 3. The relationship between the water content and the water activity was independent of whether the final state was reached by compaction or swelling. Excellent agreement was also found with the results of the adsorption isotherm, indicating that the capillary effects, presumably responsible for the hysteresis in adsorption-desorption cycles, are essentially felt during the desorption process, as discussed in Gregg and Sing (1982). Glaeser and Méring (1968) investigated the microscale swelling of Ca-smectite by XRD. Their results show that the transition between one and two layers of adsorbed water correspond to a water activity of 0.2, whereas osmotic swelling starts for aw > 0.90. Most of the water activities measured in this work were between 0.4 and 0.9, indicating that crystalline behavior of the clay dominated. The large variations of aw were probably due to the partial removal of the second layer of water.

To establish a rational basis for the interpretation of the results, an osmotic coefficient, Φ, must be defined and calculated. For electrolyte solutions, Φ relates the water activity, aw, of the solution to its molality, m:

$$\ln(aw) = -(\nu\Phi/55.51)m \qquad (3)$$

where ν is the number of ions into which the electrolyte dissociates and 55.51 is the number of moles in one kilogram of pure water. As for charged membranes, the number of ions into which the electrolyte (i.e., the membrane) dissociates is not known; hence, the defi-

Table 2. Water activity measurements for the Ca smectite-$CaCl_2$ cakes.

| Pressure (bar) | Void ratio | Salt molality | | Clay molality (mole/kg) | Water activity |
		Initial[1] (mole/kg)	Cake[2] (mole/kg)		
208	0.70	1.0	0.273	3.28	0.84
520	0.59	1.0	0.393	3.87	0.67
728	0.60	1.0	0.387	3.80	0.69
1040	0.50	1.0	0.349	4.49	0.45
1560	0.49	1.0	0.252	4.67	0.42
20	1.35	3.0	2.43	1.78	0.74
40	1.21	3.0	2.20	1.98	0.73
208	0.87	3.0	1.62	2.69	0.70
416	0.61	3.0	1.40	3.83	0.61
832	0.53	3.0	1.11	4.41	0.47
1664	0.54	3.0	0.919	4.34	0.48
20	1.29	5.0	3.81	1.95	0.48
40	1.19	5.0	3.80	2.12	0.48
104	0.77	5.0	3.63	3.26	0.45
208	0.64	5.0	3.38	3.89	0.44
416	0.69	5.0	3.01	3.56	0.42
832	0.55	5.0	2.88	4.44	0.37
1664	0.57	5.0	3.13	4.35	0.30
1664	0.50	5.0	2.56	4.84	0.27

[1] Concentratoin of the initial suspending fluid.
[2] Equilibrium concentration in the cakes.

nition of Φ is modified by introducing an osmotic product, $\overline{\nu\Phi}$ (Glueckauf, 1952). The relationship between $\overline{\nu\Phi}$, aw, and the membrane molality, A, can be obtained by substitution of A for m in Eq. (3). Using the data of Table 1, the osmotic product $\overline{\nu\Phi}$ can be calculated as a function of A. The results are plotted in Figure 4 with the osmotic product for $CaCl_2$, as obtained from the data compiled in Rard *et al.* (1977). To permit comparison, the osmotic product for $CaCl_2$ was based on the chloride molality. The very sharp rise in the clay osmotic product at high molality was not observed for the $CaCl_2$ solutions, probably because of the higher hydration energy of the clay system (Keren and Shainberg, 1979). Also, the osmotic product of the clay cakes assumed very low values for concentrations. This phenomenon corresponds to the minimum observed in the osmotic product of electrolyte solutions, which is due to Debye-Hückel interactions between ions. The decrease observed for the clay is similar to that for other ion exchangers (e.g., Glueckauf, 1952; Soldano and Larson, 1954) and is probably due to the double layer interaction between the clay particles. The osmotic product should pass through a minimum for some value of A to attain, at infinite dilution, a finite value. This could not be investigated with our equipment, as very accurate determinations of water activity values close to 1 would have been required.

The above observations have some implications for the behavior of the mixed clay-$CaCl_2$ systems discussed below; their osmotic behavior should be largely controlled by the clay for large values of A, and by the co-ion concentration for low values of A.
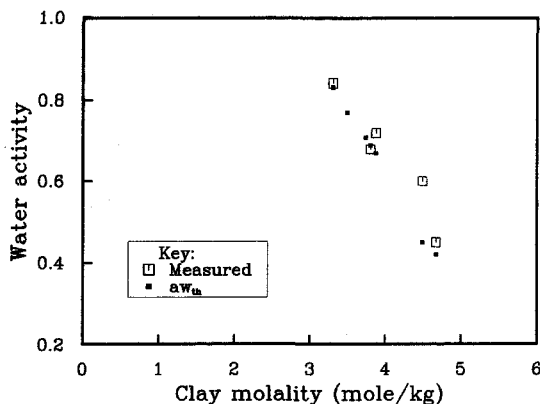
Figure 5. Water activity vs. clay molality for Redhill smectite cakes prepared in 1 M CaCl$_2$. Filled squares are data calculated assuming osmotic equilibrium.

Figure 6. Water activity vs. clay molality for the Redhill smectite cake prepared in 3 M CaCl$_2$. Filled squares are data calculated assuming osmotic equilibrium.

Ca-smectite/CaCl$_2$ systems. Three series of measurements were made using 1, 3, and 5 M CaCl$_2$ solutions as suspending fluids to prepare the clay compacts. The results of the salt concentration, water content, and water activity measurements are listed in Table 2. The salt concentration in the cakes depended strongly on the water content; substantial anion exclusion took place. The decrease is particularly strong for void ratios <0.70, corresponding to the expulsion of part the second water interlayer. Similar results were obtained by von Engelhardt and Gaida (1963) for both Na- and Ca-exchanged clays. Two new features were observed for the water activity results: (1) for the largest void ratios, the water activity of the compacted clays levelled off at a value close to the water activity, aw$_0$, of the suspending fluid (i.e., 0.75 and 0.50 for, respectively, the 3 and 5 molal solutions); (2) lower values of water activity were obtained for these systems (compared with the deionized water suspensions), particularly at the highest salt concentrations.

Clearly, the water activity of the clay-CaCl$_2$ mixtures must have been a function of the concentrations of the two components in the cakes. If P$_c$ is the pressure used to prepare a cake,

$$P_c = P_m + P_{osm}, \qquad (4)$$

where P$_m$ is a stress due to mechanical interactions between the clay particles (or the part of the compaction pressure, P$_c$, supported by the solid matrix) and P$_{osm}$ is the osmotic pressure developed between the clay phase and the external electrolyte solution produced by the filtration. For both the clay phase and the external phase the water chemical potential can be defined as:

$$\mu_i = \mu' + RT \ln(aw_i) + P_i\bar{V}. \qquad (5)$$

The subscript i designates the phase (1 for the clay, 2 for the external fluid). The reference potential μ' is defined with respect to infinite dilution, $\bar{V}$ is the molal
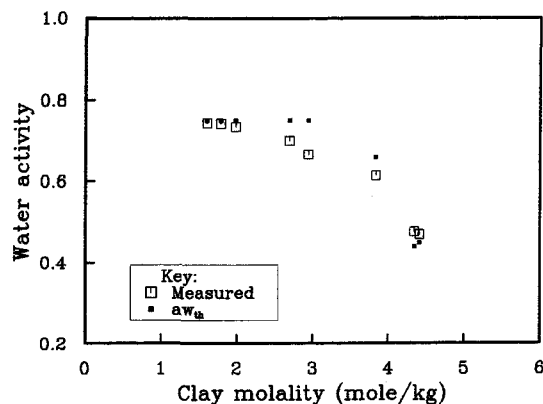
volume of water, P$_i$ is the pressure, R is the gas constant, and T is the temperature. At equilibrium

$$P_{osm} = P_1 - P_2 = (RT/\bar{V})\ln(aw_2/aw_1). \qquad (6)$$

The condition that P$_1 \geq 0$ (no cavitation) implies that:

$$aw_1 \leq aw_2\exp(P_2\bar{V}/RT). \qquad (7)$$

In our experiments, P$_2 = 1$ bar; hence, the above equation was equivalent (within experimental accuracy) to aw$_1 \leq$ aw$_2$. This condition had to be met if osmotic equilibrium was achieved during the compaction.

For electrolyte solutions, the chemical potentials, μ_i, of the individual components satisfy the Gibbs-Duhem equation:

$$\sum_i n_id\mu_i = 0. \qquad (8)$$

If, following the formalism developed for charged membranes by Glueckauf (1952), a chemical potential is introduced for the clay, Eq. (8) gives, at constant pressure and temperature:

$$-n_wd \ln(aw_1) = n_cd \ln(ac) + n_sd \ln(as). \qquad (9)$$

The water activity can be derived by integration of Eq. (9) from the reference state (infinite dilution) to the final state. The two mean activities (ac and as for the clay and the salt, respectively) are functions of both the clay and the salt molalities, but to obtain an idea of the behavior of the system, ac is assumed to equal f(A) and as is assumed to equal f(CaCl$_2$), i.e., the salt and the clay did not interact. This assumption may be justified by the fact that, in the range of concentrations covered by the experiments, activities are dominated by concentration and hydration effects. The diffuse double layer and Debye-Hückel contributions to the activities, which depend on interactions between the clays and the ionic species present in the system, will be small compared to the direct interactions of each of the species with the solvent. Eq. (9) therefore clearly leads to:
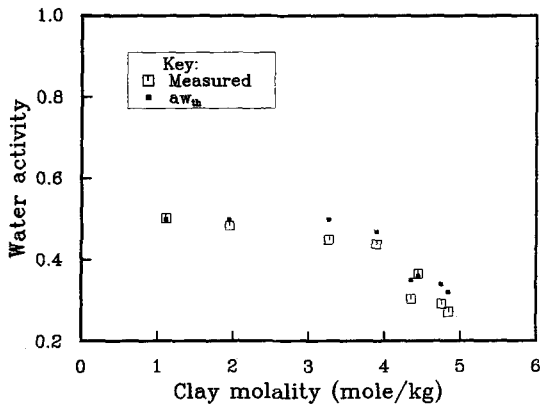
Figure 7.   Water activity vs. clay molality for Redhill smectite cake prepared in 5 M CaCl$_2$. Filled squares are data calculated assuming osmotic equilibrium.

$$-\ln(aw_1) = \int_0^A Ad \ln(ac) + \int_0^m md \ln(as). \quad (10)$$

The two integrals on the right hand side are in fact equal to the logarithms of the notional water activities, aw_c^* and aw_s^*, of a water-clay system and a CaCl$_2$ solution having the concentrations measured in the mixed system. Thus,

$$aw_1 = aw_c^* \times aw_s^*. \quad (11)$$

If equilibrium is achieved during the compaction, the water activities in the clay-CaCl$_2$ systems should satisfy $aw_1 < aw_0$ and $aw_1 \sim aw_c^* \times aw_s^*$.

The values of aw_c^* and aw_s^* can be calculated from the results of the water-clay systems and the data compiled in Rard *et al.* (1977). For the higher water contents, the product $aw_c^* \times aw_s^*$ was found to exceed slightly aw_0, which contradicts the first condition. In Figures 5–7, the measured water activities are plotted as a function of A, together with the quantity $aw_{th} = \min(aw_0, aw_c^* \times aw_s^*)$. The good agreement between the two sets of data suggests that osmotic equilibrium was obtained during the compaction and that the scaling described above for the water activity of the mixed systems held, at least for fairly compacted systems. Interestingly, the failure of the scaling at low compaction (i.e., where aw_1 slightly exceeded aw_0) corresponded to the sharp drop in the osmotic product of the clay. As inferred from the clay-water results, the behavior of the system was then controlled much more by the electrolyte concentration than by the clay content.

Compaction and swelling of the Fuller's earth core

The void ratios obtained at equilibrium for each of the pressure steps are plotted as a function of the axial stress in Figure 8. The void ratio did not drop significantly for pressures <30–50 bar, but large variations were observed at higher pressures. This change in the rate of compaction can perhaps be interpreted as an
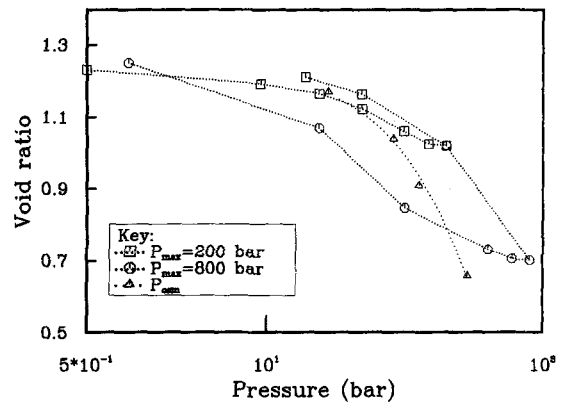

Figure 8.   Void ratios of Redhill smectite core as a function of effective axial stress. P$_{max}$ denotes *maximum pressure of each cycle*, P$_{osm}$ the osmotic pressure calculated from the data of Table 1.

indication of the depth of burial of the sediment. At 800 bar, the void ratio reached a value of 0.70, corresponding to the structure of a clay with two layers of water. For the two compaction-swelling cycles, the porosity lost in the compaction was fully recovered during swelling; however, large hysteresis loops were observed, indicating that some degree of irreversibility was present.

The results for the axial and radial strains are plotted in Figures 9 and 10, respectively. The anisotropy of the clay matrix is reflected in the results: in the axial direction, strains were as much as three times greater than in the radial direction, indicating that, as expected, the core compacted preferentially in the direction perpendicular to the bedding planes. A small increase of the diameter was detected during the cycles from both the strain data and the final measurement of the core dimensions, indicating that the small shear stresses imposed on the sample during the test caused some irreversible creep and deformation.
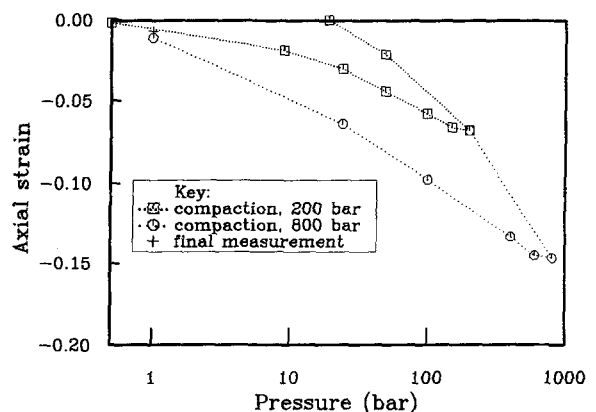
Although the compaction-swelling cycles can be

Figure 9.   Axial strain vs. effective axial stress for compaction and swelling of the Redhill smectite core. Cross indicates actual length variation measured at end of the test.
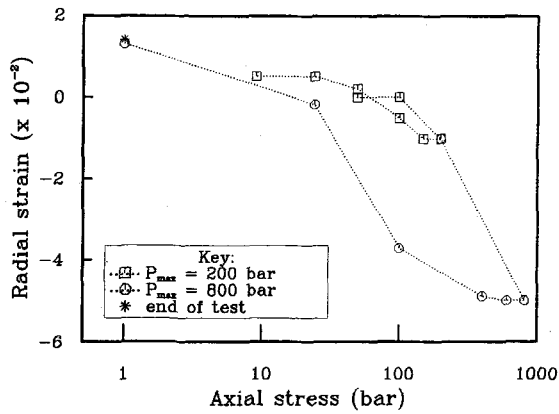
Figure 10. Radial strain vs. effective confining pressure for compaction and swelling of Redhill smectite core. Star indicates actual diameter variation measured at end of the test.

Table 3. Strains and void ratios for compaction-swelling equilibrium of a core of Redhill Ca-smectite.

Axial stress (bar)	Radial stress (bar)	Axial strain (%)	Radial strain (%)	Void ratio
20	19	0	0	1.21
50	49	−2.2	0	1.16
200	195	−6.8	−1.0	1.02
150	145	−6.6	−1.0	1.02
100	99	−5.8	−0.5	1.06
50	49	−4.4	+0.2	1.12
25	24	−3.0	+0.3	1.17
10	9	−1.9	n.d.	1.19
1.5	1	−0.2	+0.5	1.23
800	795	−14.7	−5.0	0.70
600	595	−14.5	−5.0	0.71
400	395	−13.3	−4.9	0.73
100	99	−9.8	−3.7	0.85
25	24	−6.4	−0.2	1.07
2	1.5	−1.1	+1.0	1.25[1]
2	1.5	−0.7[1]	+1.4[1]	1.25[1]

[1] Denotes values measured at the end of the test. Data above and below the line correspond to the 200-bar and 800-bar maximum pressure cycles, respectively.

nearly reversible for Li-smectite suspensions (Lubetkin *et al.,* 1984), Ca-smectite always shows very open cycles, and the swelling recovery corresponds to only a fraction of the volume lost during the consolidation phase (Olson and Mesri, 1970; Mesri and Olson, 1971). Inasmuch as a total recovery of the porosity was observed for the core of Fuller's earth, different mechanisms must have been responsible for the behavior at high- and low-clay contents. The data of Mesri and Olson show, for suspensions, the negligible contribution of osmotic forces to the compaction for e > 2. Indeed, for a given pressure, the void ratio does not depend on the electrolyte content of the suspension as expected from the DLVO theory. Certainly, the force dominant during the first compaction must have been irreversible and probably was due to mechanical friction associated with the reorganization of the clay matrix and the progressive alignment of the clay particles. On the other hand, the data obtained for the core, showing total recovery of the volume changes for e < 1.3, suggest that some reversible force was important in that range
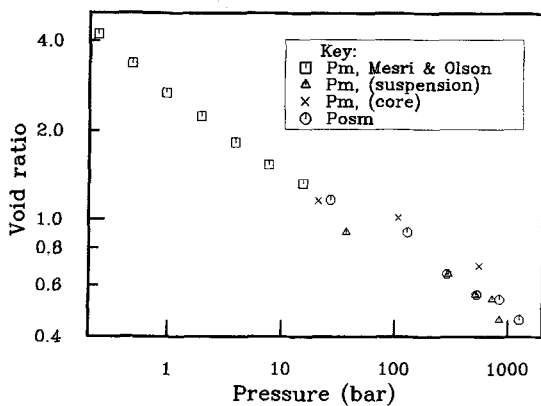

Figure 11. Relationship between matrix force, P_m, osmotic pressure, P_{osm}, and void ratio. Data for e > 2 are from Olson and Mesri (1970).

of void ratio. The osmotic pressure, P_{osm}, which developed inside the core at equilibrium, can be easily calculated from Eq. (10) and the data of Table 1. The values obtained are also plotted in Figure 8 for comparison. Over most of the pressure range, P_{osm} was intermediate between the compaction and the swelling pressures, explaining why good recovery of the initial volume was observed in the experiment. The presence of hysteresis loops indicates, however, that some degree of irreversibility was still present in the system. For compaction equilibrium, the force P_c applied on the sample was balanced by two contributions: P_{osm} and an irreversible force P_m due to the solid matrix (Eq. (4)). The osmotic pressure was also larger than the swelling pressure on part of the range investigated, suggesting that matrix forces could also restrict the swelling. Edge-to-face links are formed in clay gels that are able to sustain some stress (Norrish, 1954; van Olphen, 1954; Gueuze and Rebull, 1966). Because the strength of these bonds depends on the electrolyte concentration (van Olphen, 1954), their nature must differ from that of the resistance to compaction, inasmuch as the results Mesri and Olson (1971) show that P_m is independent of salt concentration.

The osmotic pressure can be compared directly with P_m using the data of Olson and Mesri (1970) and Mesri and Olson (1971) for calcium montmorillonite suspensions to estimate P_m for e > 2, assuming no osmotic contribution in the resistance to compaction. For smaller void ratios, the data of Table 1 can be used by subtracting P_{osm} from the compaction pressure P_c. The results are plotted in Figure 11 along with the values of P_{osm}. Clearly, the data of Mesri and Olson (1971) are consistent with those of the present report: a single

power law relationship could easily be fitted through the values found for P_m from the two data sets. The values of P_m for the core compaction were somewhat larger than those for suspension. This additional resistance could have been due to the cementation of the undisturbed rock. Surprisingly, the osmotic pressure assumed values very close to those of P_m for $e < 1$. Unfortunately, the range of P_{osm} was restricted by the accuracy of the water activity measurement, and direct confirmation of the fact that this force was small compared with P_m for void ratios > 2 cannot be made using the present data.

SUMMARY AND CONCLUSIONS

The osmotic properties of the system water-$CaCl_2$ Ca-smectite were determined over a wide range of compositions and were in good agreement with the results of vapor adsorption. Substantial anion exclusion was observed if $CaCl_2$ was added. The presence of salt significantly affected, at high concentrations, the water activity of the compacts. The experimental values of water activity were modelled using a semi-empirical law, assuming that osmotic equilibrium had been achieved. The compaction and swelling behavior of a core of Fuller's earth showed that the material recovered volume changes for void ratios < 1.25. The deformation was clearly anisotropic, the strains being larger in the direction perpendicular to the bedding planes. The hysteresis loops described by the material during compaction-swelling cycles can be explained if, in addition to the osmotic pressure, a mechanical force opposed the compaction restrained swelling. An estimate of the force opposing compaction was in agreement with those derived from the data for Ca-montmorillonite suspensions by Mesri and Olson (1971).

Although these data are limited to a particular Ca-smectite, systems containing only one cation (e.g., NaCl-Na smectite) should have similar properties. Further degrees of complexity would have to be introduced if the simultaneous presence of several salts (in order to take into account the effect of cation exchange with the clay) and the presence of several minerals susceptible to interaction with water were to be considered.

ACKNOWLEDGMENTS

REFERENCES

Attard, P., Mitchell, J. D., and Ninham, B. W. (1988) Beyond Poisson-Boltzmann: Images and correlations in the electric double layer II: *J. Chem. Phys.* **89**, 4358–4367.

von Engelhardt, W. and Gaida, K. H. (1963) Concentration changes of pore solutions during the compaction of clay sediments: *J. Sed. Pet.* **33**, 919–930.

Glaeser, R. and Méring (1968) J. Homogeneous hydration domains of the smectites: *Compt. Rend. Acad. Sci. (Paris)* **267**, 436–466.

Glueckauf, E. (1952) A theoretical treatment of cation exchangers. I: *Proc. Roy. Soc. London* **A214**, 207–225.

Gregg, S. G. and Sing, K. S. W. (1982) *Adsorption, Surface Area and Porosity:* Academic Press, London, 126–132.

Gueuze, E. C. W. A. and Rebull, P. M. (1966) Mechanical force fields in a clay mineral particle system: in *Clays and Clay Minerals, Proc. 14th Natl. Conf., Berkeley, California, 1965*, S. W. Bailey, ed., Pergamon Press, New York, 103–116.

Hunter, R. J. (1987) *Foundations of Colloid Science, Vol. 1:* Oxford University Press, Oxford, United Kingdom.

Israelachvili, J. N. and Adams, G. E. (1978) Measurements of forces between two mica surfaces in aqueous electrolyte solutions in the range 0–100 nm: *J. Chem. Soc. Faraday Tans. 1* **74**, 975–1001.

Keren, R. and Shainberg, I. (1979) Water adsorption isotherms and heat of immersion of Na/Ca montmorillonites systems—II: mixed systems: *Clays & Clay Minerals* **27**, 145–151.

Kjellander, R. and Marčelja, S. (1988) Attractive double-layer interactions between calcium clay particles: *J. Colloid Interface Sci.* **126**, 194–211.

Kjellander, R., Marčelja, S., Pashley, R. M., and Quirk, J. P. (1988) Double-layer correlation forces restrict calcium-clay swelling: *J. Phys. Chem.* **92**, 6489–6492.

Lubetkin, S. D., Middleton, S. R., and Ottewill, R. H. (1984) Some properties of clay-water dispersions: *Phil. Trans. R. Soc. Lond. A* **311**, 353–368.

Mesri, G. and Olson, R. E. (1971) Consolidation characteristics of montmorillonite: *Géotechnique* **21**, 341–352.

Norrish, K. (1954) The swelling of montmorillonite: *Disc. Faraday Soc.* **18**, 120–134.

van Olphen, H. (1954) Interlayer forces in bentonite: in *Clays and Clay Minerals, Proc. 2nd Natl. Conf., Columbia, Missouri, 1953*, Ada Swineford and Norman Plummer, eds., Natl. Acad. Sci. Natl. Res. Conf. Publ. 327, Washington, D.C., 418–438.

van Olphen, H. (1977) *An Introduction to Clay Colloid Chemistry:* Wiley, New-York, 29–42, 92–108.

Olson, R. E. and Mesri, G. (1970) Mechanism controlling compressibility of clays: *J. Soil. Mech. Found. Div.* **96 SM6**, 1863–1878.

Pashley, R. M. (1981) Hydration forces between mica surfaces in Li, Na, K, and Cs electrolyte solutions: *J. Colloid Interface Sci.* **80**, 153–162.

Pashley, R. M. and Israelachvili, J. N. (1984) Molecular layering of water in thin films between mica surfaces and its relation to hydration forces: *J. Colloid Interface Sci.* **101**, 511–523.

Rard J. A., Habenschuss, A., and Spedding, F. H. (1977) A review of the osmotic coefficients of aqueous $CaCl_2$ at 25°C: *J. Chem. Eng. Data* **22**, 180–186.

Robinson, R. A. and Stokes, R. M. (1970) *Electrolyte Solutions:* Butterworth, London, p. 510.

Söhnel, O. and Novotný, P. (1985) *Densities of Aqueous Solutions of Inorganic Substances:* Elsevier, Amsterdam, p. D225.

Soldano, B. and Larson, Q. V. (1954) Osmotic behavior of anion and cation exchangers: *J. Phys. Chem.* **77**, 1331–1334.

Young, J. F. (1967) Humidity control in the laboratory using salt solutions—a review: *J. Appl. Chem.* **17**, 241–245.

Warkentin, B. P., Bolt, G. H., and Miller, R. D. (1957) Swelling pressure of montmorillonite: *Soil Sci. Soc. Amer. Proc.* **21**, 495–497.